Improving Extended Kriging with Chapman Model and Exponential Variation Function Model

Pan Liu and Rui Li

Abstract In the satellite-based augmentation system, the ionospheric error as one of the main error sources has a big influence on the navigation capability of single frequency user. At present, the IGD is estimated based on the distance-weighted algorithm and Kriging plane fitting algorithm with a single-layer shell model, in which ionosphere is equivalent to a thin shell at certain height. However, the error introduced by single-layer thin shell model leads to a poor precision of ionospheric delay estimation. In terms of this issue, some scholars proposed extended Kriging algorithm based on empirical model, but the accuracy is not high and are limited by experience. This paper proposes an extended tomography algorithm improving the estimation precision of extended Kriging algorithm using Chapman model instead of empirical model, and fitting the single Gaussian random delays. The analysis is made using ionospheric data collected from WAAS reference stations and CORS stations within the scope of the United States in this paper. First, we compare the fitting accuracy of Kriging algorithm and extended algorithm on each reference station, and analyze the improvement under the different ionospheric disturbance conditions and elevation angles. Then we compare the fixed delays based on the two methods. The results show that the fitting precision of the improved algorithm is increased by 10–50 %, especially in the case of low elevation angle, and the UIVE is also reduced by 5–40 %.

Keywords SBAS · Grid ionospheric correction · Tomography

P. Liu (✉) · R. Li
Beihang University, Beijing, China
e-mail: liupanlzu@yeah.net

R. Li
Collaborative Innovation Center of Geospatial Technology, Wuhan, China

J. Sun et al. (eds.), *China Satellite Navigation Conference (CSNC) 2016 Proceedings: Volume II*, Lecture Notes in Electrical Engineering 389,
DOI 10.1007/978-981-10-0937-2_15

1 Introduction

In the satellite-based augmentation system, the ionosphere error as the one of main error sources has a big influence on the navigation capability of single frequency user. At present, the widespread adoption of single-layer shell model calculate ionospheric grid to analysis the ionospheric characteristics between the reference stations and satellites. Wide area augmentation system (WAAS) and European Geostationary Navigation Overlay Service (EGNOS) using Kriging plane fitting and distance-weighted algorithm, respectively, to estimate the ionospheric delay at grid points, then broadcast ionospheric grid delay (IGD) and grid ionospheric vertical delay error (GIVE) to user. Finally, user selects near three or four grid points near IPP to calculate slant delay and confidence bound in user propagation path by bilinear interpolation to ensure the user's positioning accuracy and integrity.

But due to the large fluctuations of ionospheric in the solar geomagnetic storms, traditional single-layer shell method sets the ionosphere at the fixed height and hardly considers the ionospheric electron density in the vertical direction, so the accuracy is affected. In terms of this issue, some scholars proposed extended Kriging algorithm based on empirical model [1], but the accuracy is still limited because of the empirical coefficient listed in Table 1. This paper proposes an extended algorithm improving the estimation precision using Chapman model, which establishes a more accurate ionosphere model.

The algorithm analysis is made using ionospheric data collected from WAAS reference stations in this paper. First, we analyze both the estimation accuracy of different algorithms on each reference stations, and the improvement under different ionospheric disturbances and different elevations. Then we take the operational reference station continuously (CORS) stations as the users, and compare the slant delay values and confidence bound calculated by the three algorithms.

2 Ionospheric Delay Estimation

2.1 Extended Kriging Algorithm

Extended Kriging algorithm is mainly proposed by Juan blanch, which takes the ionospheric electron concentration in vertical direction and the distance correlation of the delay values into account, and introduces Gaussian random fields to establish multilayer thin shell structure based on the Kriging algorithm. This algorithm combines the advantages of Kriging algorithm and tTomography algorithm.

Table 1 The ionospheric coefficient of Empirical model

High (km)	350	400	450	500	550	600	650
φ_k	0.25	0.125	0.125	0.125	0.125	0.125	0.125

A p layers model is introduced instead of the single-layer thin shell, and a weighting factor ϕ_k is given to the k layer to describe the average weight of the electron concentration. The weighting factor are listed in Table 1, and:

$$\sum_k \varphi_k = 1 \tag{1}$$

As a regional model is established in each single layer, the ionospheric delay value can be equivalent to a mean value m plus a multidimensional Gaussian random field $r_k(x)$ dependent on the position of ionospheric pierce point x, assuming that Gaussian random fields of the layers are independent and identically distributed. Therefore, the vertical delay value of the k layer is equivalent to

$$I_{v,k} = \varphi_k \cdot (m + r_k(x)) \tag{2}$$

And the slant delay of the i measured on the k layer at the reference station is as follows:

$$I_{s,i} = \sum_{k=1}^{p} \varphi_k \cdot (m + r_k(x_{k,i})) \cdot ob_{k,i} \tag{3}$$

where $ob_{k,i}$ is the relative slant factor. Since r_k is independent of each other in different layers, the covariance of the projection values of the two propagation paths is given by

$$\begin{aligned} \operatorname{cov}(I_{s,i}, I_{s,j}) =& E\left(\left(\sum_{k=1}^{p} \varphi_k \cdot r_k(x_{k,i}) \cdot ob_{k,i}\right)\left(\sum_{k=1}^{p} \varphi_k \cdot r_k(x_{k,j}) \cdot ob_{k,j}\right)\right) \\ =& \sum_{k=1}^{p} \varphi_k^2 ob_{k,i} ob_{k,j} \operatorname{cov}\left(r_k\left(x_{k,i}\right), r_k\left(x_{k,j}\right)\right) \end{aligned} \tag{4}$$

Neglecting the measurement noise, the vertical delay value of grid point can be calculated using Kriging algorithm with Eq. (4), and then broadcasted to users. However, the vertical direction of the extended Kriging is limited by the fixed coefficient model, the improved accuracy is not high, and the specific coefficients are not given.

2.2 Improved Extended Algorithm

2.2.1 Chapman Model

Because of the ionospheric electron concentration is affected by solar activity, geomagnetic activity, season and time of day, a complete the theoretical analysis is

too complicated, so that we often established basic parameters to construct the empirical model of the ionosphere based on a large number of observations. The functions of the models include the Chapman function, the spherical harmonic function, and so on [2]. There are also many empirical models to choose from, which mainly include the international reference ionosphere model (IRI) and the parametric ionospheric model (PIM) [2].

The Chapman function is used to describe the distribution of electron density in the vertical direction, and the peak height of the electron density is obtained according to the changes of the atmospheric composition and the state of the sun, in which the electrons in the ionosphere are mainly concentrated between 100 and 1000 km. According to the IRI and the PIM models, we select the electron concentration peak model of the 450 km, as shown in the Chapman layer (Fig. 1):

Specific expressions are as follows:

$$\mathrm{Ch}(h, H_k) = \exp\left(1 + \frac{h_k - h}{H_k} - \exp\left(\frac{h_k - h}{H_k}\right)\right) \tag{5}$$

where, the peak point is h_k = 450 km, the model height is H_k = 90 km. The peak height of single-layer shell in WAAS is 350 km (Table 2).

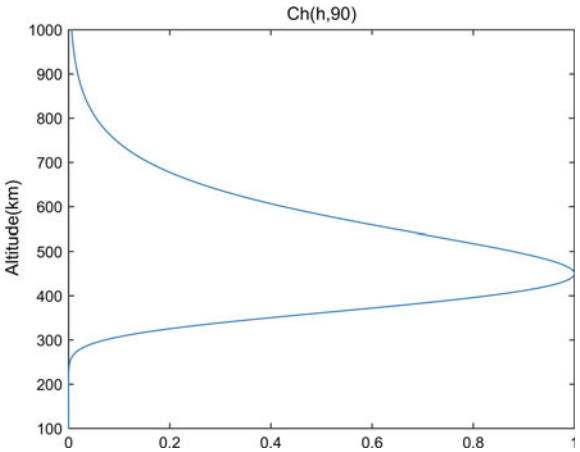

Fig. 1 Chapman layer

Table 2 The ionospheric coefficient of Chapman model

High (km)	360	450	540	630	720	810
φ_k	0.18	0.37	0.26	0.12	0.05	0.02

2.2.2 Exponential Variation Function Model

Ionospheric delay value varies slowly with time and the geographic location, so that the closer ionospheric pierce points have a higher correlation value in the thin shell model. So the ionospheric delay value is a special random variable, which is related to the location of the position. Because of the failure of the traditional probabilistic analysis method in describing the characteristics of delay value completely, the geostatistics variogram are introduced in single-layer shell Kriging, quantitatively describing spatial correlation of regionalized variables, and achieve better results [3].

This paper establishes a multilayer variation function model based on hierarchical technologies, which describe the characteristics of different propagation paths. Due to the delay value difference is 0 when the propagation paths are overlap (the delay value of the pierce point may have a larger deviation at the same position in single-layer shell), it overcomes the nugget effect (the discontinuity of starting point) in single-layer shell Kriging.

In each layer, the mean m of the delay value is deterministic as a plane trend term, so we only analyze the random items $r_k(x)$ in the delay value. Using the first-order plane fitting, we obtain the fitting coefficient by the least square method, and construct the difference of random entry to establish the corresponding experimental variation function.

The main steps are:

1. In the k layer, we obtain the position of the geometrical center at each pierce point pair for all the pierce points as the data source. The trend coefficient is obtained by all the points, except the selected pierce point pair, within the circle of radius 1200 km.
2. The mean value of the delay (m_i, m_j) is calculated using the fitting coefficient, and the difference of the slant delay value of the current layer $(I_{s,i} * \varphi_k, I_{s,j} * \varphi_k)$ is calculated.
3. The difference between the p layer and the random term of the space is obtained by $\Delta r_{ij} = \sum_{k=1}^{p} r_k(x_{k,i}) - \sum_{k=1}^{p} r_k(x_{k,j})$.
4. The random entry differences of all the points in the plane are obtained by traversing. We obtain the variation function values by the distance as the independent variable, then to carry on the drawing.

In this paper, we select 6 day's data with different ionospheric disturbances index Kp listed in Table 3 for analyzing. The results are shown in Fig. 2.

Table 3 Ionospheric disturbances index of Kp

Date	03.17	04.15	06.20	06.23	06.30	07.31
Kp	8	1	1	7	2	3

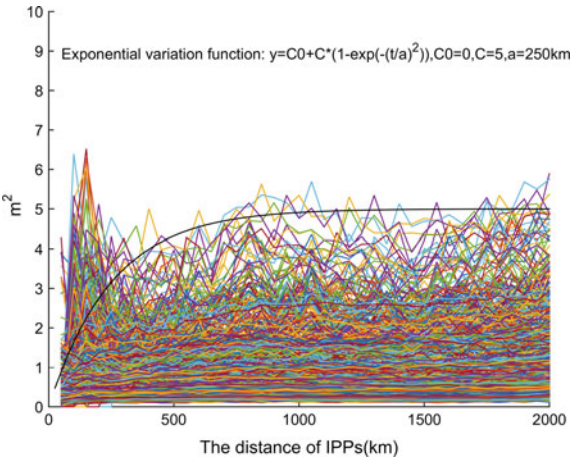

Fig. 2 Exponential variation function

According to the trend of the variation function, we select the experimental model variation function $\gamma(d) = C * (1 - \exp(-d/a))$ which is the black line, so the corresponding variance function is

$$\operatorname{cov}\left(r_k(x_i), r_k(x_j)\right) = f\left(\left\|x_i - x_j\right\|\right) = 5 \cdot \exp\left(-\frac{\left\|x_i - x_j\right\|}{250}\right) \tag{6}$$

2.2.3 The Calculation of Delay Value

According to the extended Kriging algorithm by Juan Blanch, we introduce the Chapman model and the exponential model of the regional variables above and calculate the vertical delay value of the grid points by Kriging algorithm [4]. Since the ionosphere estimation technique is linear, the slant delay value of the arbitrary propagation path is a linear combination of the measured values within a certain range. Assuming that there are n valid measurements, the ionosphere delay value is computed as follows:

$$\hat{I}_{\text{unknown}} = \sum_{i=1}^{n} \lambda_i \tilde{I}_{\text{mean},i} \tag{7}$$

As it meets the least mean square error criterion, the solution of the weighting coefficient is similar to that of Kriging method:

$$\lambda = (W - WG(G^{\mathrm{T}}WG)^{-1}G^{\mathrm{T}}W)c + WG(G^{\mathrm{T}}WG)^{-1}X_{\text{unknown}} \tag{8}$$

By solving Eq. 8, we obtained the weighted coefficients λ_i and the vertical delay value of the grid points can be calculated by Eq. 7.

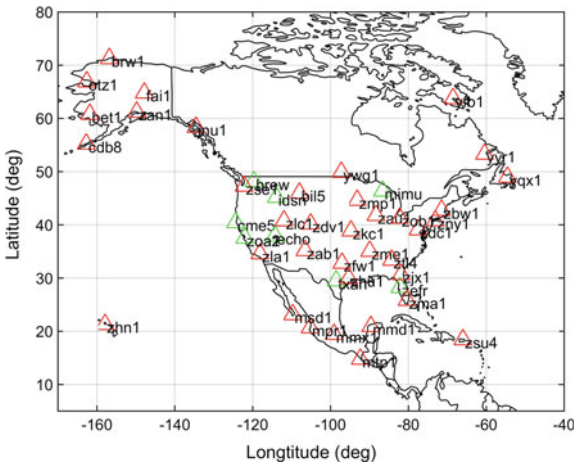

Fig. 3 The location of reference station

3 Algorithm Analysis and Results

The algorithm simulation is made using different disturbance ionospheric measurement data which collected from 38 WAAS reference stations and 8 CORS stations (red triangles and green triangles in Fig. 3, respectively) in 3 days of 2015. The cut-off angle of reference station observation takes 15° in improved algorithm, we select the delay values around 1200 km to estimate the point as the center of the circle, the minimum number of observation points is 10, and each layer of the pierce point data were selected in accordance with the 360 km.

3.1 Accuracy Analysis of Estimation Algorithm

We use the method of data deprivation to fit the remaining measurement pairs except the pair of satellite and station we selected, and then contrast the real value and the estimated value. In order to guarantee the accuracy of the algorithm, we excluded the data which have the same reference station with the estimated pair. At first, the root mean square and maximum of error to analyze the fitting accuracy of the planar Kriging algorithm, extended Kriging algorithm, and the improved algorithm, the results are as follows (Table 4).

Table 4 The error analysis between the three algorithms

	2015.06.20		2015.07.31		2015.03.17	
	RMS (m)	Max (m)	RMS (m)	Max (m)	RMS (m)	Max (m)
Kriging	0.427	14.069	0.431	6.172	0.817	19.783
Extended kriging	0.311	4.081	0.341	3.039	0.600	7.747
Improved algorithm	0.301	4.046	0.330	2.950	0.565	7.389

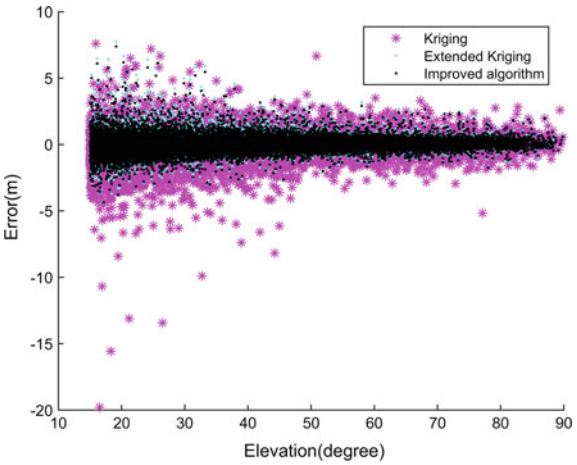

Fig. 4 The fitting errors of three algorithms

The ionospheric disturbance index Kp of the selected days are 1, 3 and 8, respectively. According to the results, we can see that the improved algorithm has a certain improvement in the fitting error.

Next we analyze the WAAS station fitting error condition in March 17th Fig. 4 is the comparison of the three algorithms, it can be seen that the improved method of fitting error value has a certain decrease especially in the case of low elevation, but there are also some larger errors. We list four reference stations in different locations to compare root mean square errors of the three algorithms in Fig. 5. The improved algorithm has an obvious improvement compared with the Extended Kriging algorithm and Kriging in the reference station at the center position

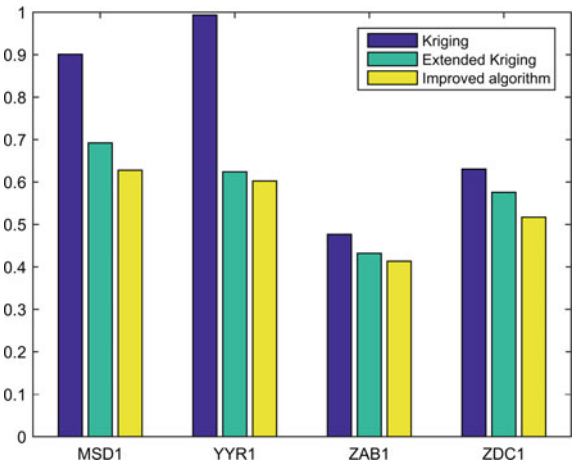

Fig. 5 Error variance histogram of reference stations

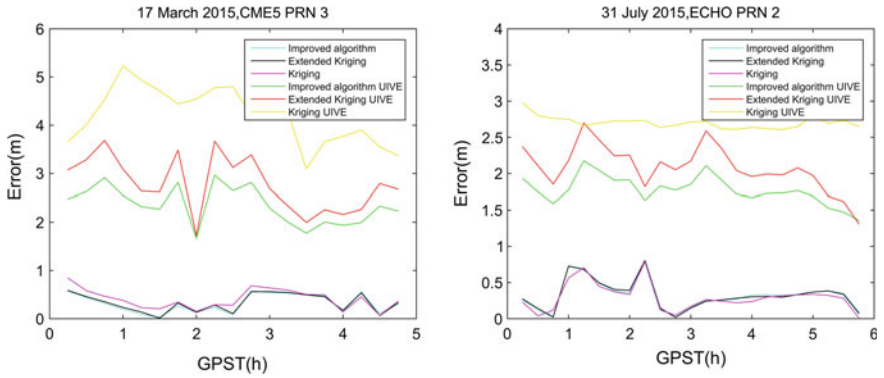

Fig. 6 IGD error and UIVE comparison of three algorithms

(ZAB1, ZDC1) and the edge position (MSD1, YYR1) of CONUS. But because the center location has lager quantity data, the model accuracy of three methods are similar, so the improvement is not obvious.

In summary, the improved algorithm has an improvement contrasted with Kriging and Extended Kriging especially in low elevation, and the fitting accuracy is improved by an average of 50 and 5 % compared with Kriging and Extended Kriging, respectively.

3.2 User Grid Correction Analysis

This paper selects 8 CORS stations as users plotted in Fig. 3, we interpolated the grid point delay values by WAAS measurement in the same time, and compared the accuracy of three algorithms by the difference between truevalue and its fitted value. We choose continuous observation of GPS satellite PRN 3 collected by station CME5 on March 17th when the Kp is 8 and GPS satellite PRN 2 collected by station ECHO on July 31st when the Kp is 3 to demonstrated in Fig. 6.

From Fig. 6 and Table 3, the improved algorithm is more fit for the user error bounding than Kriging, and the average reduction of UIVE is more than 40 %. Compared with Extended Kriging, improved algorithm also has some improvement, UIVE is reduced by 5 %. The UIVE bounding possibilities of the all three algorithms are all greater than 99.9 %, and the difference of the delay value is close and the root mean square differences reach a thousand points (Table 5).

Table 5 The correction performance of the three algorithms

Date	Kriging		Extended kriging		Improved algorithm		Reduction in kriging UIVE (%)	Reduction in extended UIVE (%)
	Error RMS (m)	UIVE bounding (%)	Error RMS (m)	UIVE bounding (%)	Error RMS (m)	UIVE bounding (%)		
03.17	0.453	99.98	0.463	99.94	0.466	99.94	44.7	8.2
06.30	0.303	100	0.304	100	0.304	99.98	43.2	2.8
07.31	0.347	100	0.349	99.95	0.350	99.95	41.6	3.3

4 Conclusion

This paper propose an ionospheric shell improved algorithm combining Chapman model and exponential variation function based on the Extended Kriging algorithm, to improve the fitting accuracy especially in low elevation and severe ionospheric disturbance condition. First, we use the observation data of the WAAS reference station in the continental United States to evaluate the accuracy of the three algorithms by the differences between the real value and the fitting estimate value. Then, we take CORS stations as users to validate error bounding.

The results indicate that the estimation accuracy of improved algorithm is improved by about 20–60 % than Kriging algorithm under the different Kp index, and improved by about 5 % than extended Kriging algorithm. However, the improvement is not obvious for the center station. At the end of the user, the three algorithms has nearly the same estimation accuracy, but the mean reduction percentage of UIVE is about 40–5 % for Improved algorithm over the Kriging algorithm and extended Kriging. In the vertical direction, the Chapman model we adopted is more flexible than extended Kriging. And we take the six layers Chapman model in which the peak value is 450 km, so the computational complexity has been reduced, while the accuracy has still been improved.

References

1. Blanch J, Walter T, Enge P (2004) A new ionospheric estimation algorithm for SBAS combining kriging and tomography. In: Proceedings of the institute of navigation national technical meeting
2. Hansen AJ (2002) Tomographic estimation of the ionosphere using terrestrial GPS sensors. ProQuest dissertations and theses; Thesis—Stanford University
3. Fengqiu J, Huan Zhigan SB (2010) Estimation method of ionospheric delay of IGP based on spatial variability. J Telemetry, Tracking Command, 31(4)
4. Blanch J (2004) Using kriging to bound satellite ranging errors due to the ionosphere. ProQuest dissertations and theses; Thesis—Stanford University